Enhanced magnetoresistance in molecular junctions by geometrical optimization of spin-selective orbital hybridization

Supporting information

David Rakhmilevitch[1], Soumyajit Sarkar[2], Ora Bitton[3], Leeor Kronik[2], and Oren Tal[1]

1. Department of Chemical Physics, Weizmann Institute of Science, Rehovot, Israel
2. Department of Materials and Interfaces, Weizmann Institute of Science, Rehovot, Israel
3. Department of Chemical Research Support, Weizmann Institute of Science, Rehovot, Israel

I. Device fabrication and introduction of molecules.

The break junction samples were fabricated on phosphor-bronze substrates, spin coated with a 2-μm thick dielectric polyimide layer. Contact pads and leads were patterned using photolithography and evaporation of a 10 nm thick chrome layer followed by an 80 nm thick gold layer. The constriction was patterned using e-beam lithography followed by evaporation of an 80 nm thick nickel layer. The polyimide layer below the constriction was under-etched using inductively coupled plasma to form a freely suspended region of about 320 nm. The device was mounted into a vacuum chamber equipped with a three point bending mechanism. All AMR measurements were performed after cooling the chamber to 5.9 K. The constriction was narrowed to form an atomic junction by bending the substrate using a combination of a screw-nut mechanism for rough adjustments and a piezo-element for fine-tuning. AMR measurements were performed using a conventional lock-in current-bias scheme, while a voltage-bias lock-in technique was used for inelastic electron spectroscopy measurements. Benzene molecules (Sigma Aldrich, Anhydrous, 99.8%) were introduced to the junction using a molecular source composed of heated vacuum tube, connecting a benzene reservoir held at room temperature to a funnel right above the junction. The benzene was further purified in-situ by several freeze-pump-thaw cycles before admission of molecules to the junction.

II. The role of magneto-elastic effects

Ferromagnetic metals deform under applied magnetic field, an effect referred to as magnetostriction. Despite this being a rather small effect[1] ($\frac{\Delta l}{l} \sim 10^{-5}$), it was previously shown that nano-contacts, created by electro-deposition or by breaking a macroscopic ferromagnetic wire, can deform by orders of tens of nanometers, resulting in over 1000% variations in conductance across the junction[2]. However, experiments performed on lithographically defined break junctions in which metallic ferromagnetic films are anchored to a rigid substrate, indicated that such deformations can be negligible, allowing the detection of AMR in the order of 10% in agreement with related calculations[3]. This was further verified by demonstrating a clear

suppression of magnetostriction upon reduction of the length of the freely suspended region at the center of a ferromagnetic junction[4].

In order to diminish possible magnetostrictive effects in our experiments, the ferromagnetic section of the junction was constrained to less than 10 μm in length, along the junction axis. More importantly, the freely suspended region was reduced to less than 300 nm, as described in section I. The insignificant role of magnetostriction in our measurements was verified by several independent observations:

(1) Magneto-conductance measurements taken in the tunneling regime after breaking the contact and before the introduction of molecules did not exhibit any systematic change in conductance (Fig. S1a). This observation is in contrast to the expected high sensitivity of conductance in the tunneling regime to magnetostriction-induced variations in the distance between the electrodes of the examined junctions.

(2) The conductance response of our Ni atomic junctions to magnetic field applied in parallel and perpendicular to the junction has comparable amplitude (Fig. S3), suggesting that longitudinal deformations play a minor role.

(3) Magneto-conductance measurements in the single atom contact regime resulted in a conductance change of less than 10% (Fig. S1b), which is comparable to results, obtained previously on both Ni atomic contacts without a freely suspended region[5] and permalloy atomic contacts[6].

(4) Following the introduction of molecules to the Ni junction, we measured a non-monotonic magneto-conductance trend in response to junction elongation (Fig. 3b of the main text). This observation is consistent with negligible magnetostriction contribution. This is because the latter is expected to yield a monotonic increase in the magneto-conductance ratio as

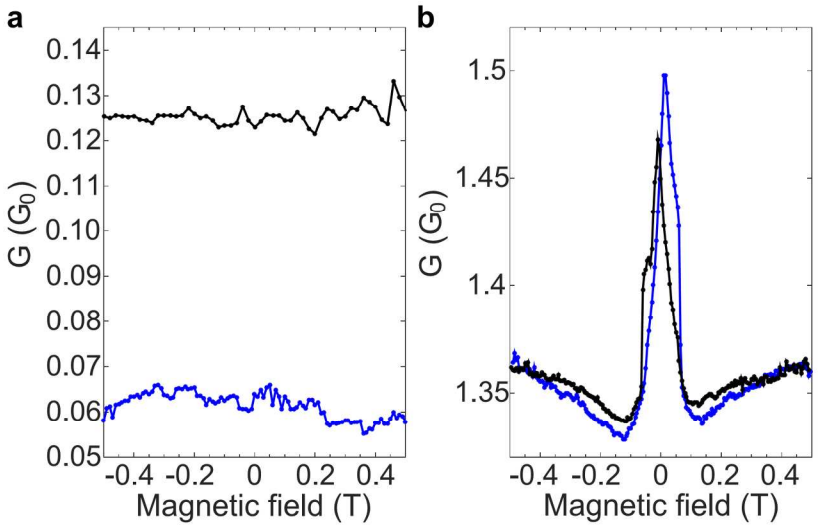

Figure S1: Magnetoconductance of Ni junctions measured in the tunneling regime (a) and in the atomic contact regime (b). The measurements were taken on different junctions.

the conductance is reduced towards the tunneling regime and the conductance sensitivity to interelectrode distance is increased.

III. AMR measurements in a rotating magnetic field.

To establish the AMR origin of the observed change in conductance with magnetic field, conductance measurements were performed while rotating a magnetic field of 0.3 T in the plane of the junction (See Fig. S2a). The chosen magnetic field amplitude is above the field required to saturate the magnetization of the electrodes. This measurement scheme is less appealing since itis susceptible to sharp variations in the measured conductance, possibly due to atomic rearrangements[7]. Figure S2b presents the conductance of an atomic junction as a function of magnetic field angle relative to the junction axis. The overall changes in conductance are in agreement with the measured values obtained by sweeping the field along the axis. However, in contrast to the latter measurement scheme, abrupt conductance variations can be observed in Fig. S2b, leading to a less reliable determination of the magneto-conductance amplitude.

Figure S2c presents the measured conductance for two independent Ni/benzene molecular junctions, exhibiting an increase in conductance when the field is directed at an angle of $45<\theta<135$ with respect to the junction axis. This angular dependence points to an AMR origin for the observed behavior, excluding other origins such as tunneling magnetoresistance**.**

IV. Determination of the easy axis of the junction.

The easy axis of the junction was determined from the conductance response of the junction to a magnetic field applied in different directions[8] as presented in Fig. S3. When the magnetic field

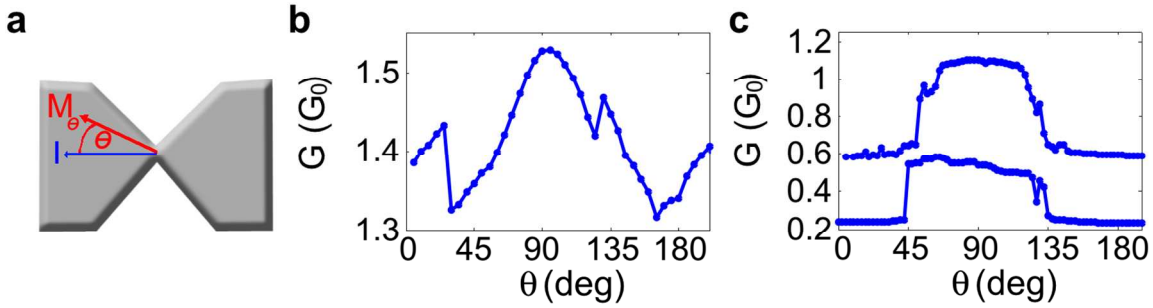

Figure S2: Conductance measurements as a function of a rotating magnetic field. (a) Schematic illustration of the relative direction of magnetization and current during the measurement. Measurements of magneto-conductance of a Ni atomic junction (b) and two different realizations of molecular junctions (c).

was swept either along the junction axis (z axis; Fig. S3a) or out of the junction plane (y axis; Fig. S3b), conductance variations in the order of 7% were observed, in agreement with previously reported results5. The conductance response to a magnetic field in the plane of the junction and perpendicular to its axis (x axis; Fig. S3c) exhibited a different behavior. In contrast to the monotonic change of conductance as the magnetic field was increased along the z or the y axis, during this measurement the conductance was rather insensitive to the applied magnetic field with minor features near zero magnetic field. This behavior is consistent with spontaneous magnetization of the junction along the x direction[9]. Applying a magnetic field in this direction preserves the perpendicular orientation of magnetization with respect to the current throughout the measurement, except near zero magnetic field where the magnetization switching occurs. Since the angle between the magnetization and the current does not vary, no systematic changes in the conductance are expected, as indeed seen in Fig. S3c. While shape anisotropy can lead to an easy axis along the z axis, we assign the observed orientation of spontaneous magnetization to the stress applied on the ferromagnetic film due to the breaking process. We note that a transverse in-plane spontaneous magnetization of a Ni thin film of a similar width under tensile stress was also shown previously[10].

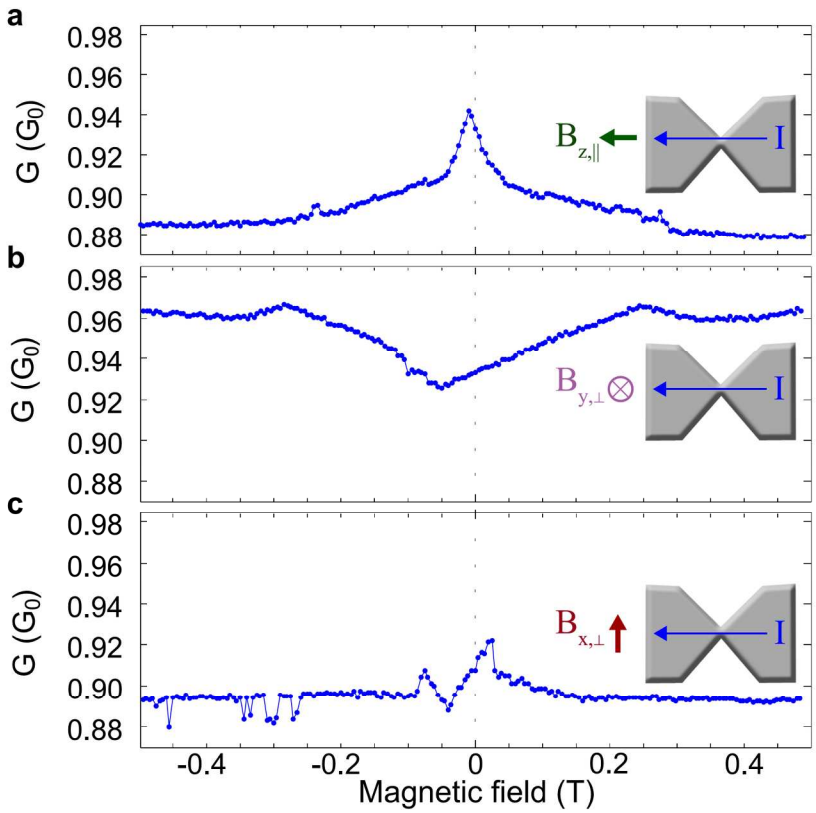

Figure S3: Conductance measurements as a function of magnetic field along the three axes of the junction as defined in the insets. The measurements were performed for Ni\benzene junctions in a stable, compact configuration.

V. Establishing transport through the molecule using inelastic electron spectroscopy:

In order to verify that the introduction of benzene to the Ni sample indeed formed molecular junctions, we performed inelastic electron tunneling spectroscopy (IETS) to look for the signature of molecular-junction vibrations. Figure S4 presents an example for the measured normalized IETS signal before and after the introduction of molecules. The feature around zero-bias observed in both graphs is attributed to excitation of phonons and magnons in the metallic electrodes[11], on top of energy-dependent variations in the electronic density of states of the point contact. However, after the introduction of molecules we observed IETS peaks around a bias voltage of 53 ± 3 mV. Similar features were previously shown to arise from vibration-induced electron scattering in benzene-based molecular junctions[12,13,14].

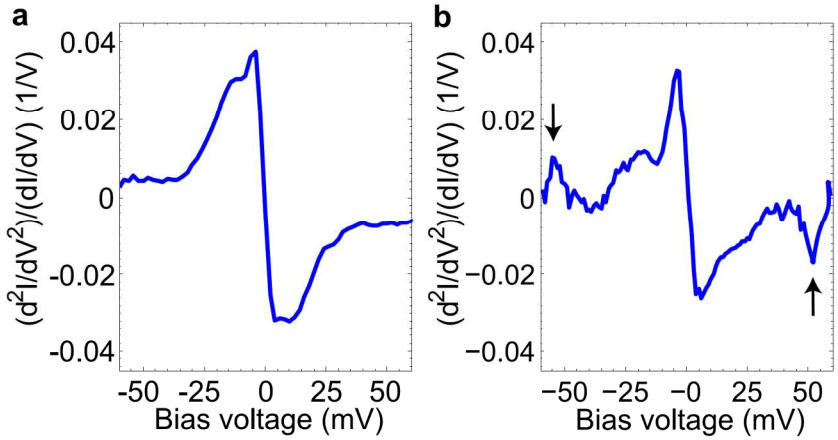

Figure S4: Differential conductance measurements taken on a Ni atomic junction before (a) and after (b) the introduction of molecules. Arrows indicate the onset voltage for vibration activation.

VI. Effects of variable molecular configurations.

The multitude of different metal-molecule configurations suggests some inherent variability in the magneto-transport properties of the junctions. Out of the 43 junctions we examined, 6 exhibited magnetoresistance higher than 150%, while the average magnetoresistance value was 58.9%. This means that while configurations with extremely high AMR are robust and reproducible they occur less often.

The effect of the molecular configuration on the measured AMR is even more evident when examining the influence of junction elongation, as exemplified by the non-monotonic AMR response in Figure 3 in the main text. Such non-monotonic behavior was observed in about 60% of the successfully-elongated junctions, some of which are shown in figure S5.

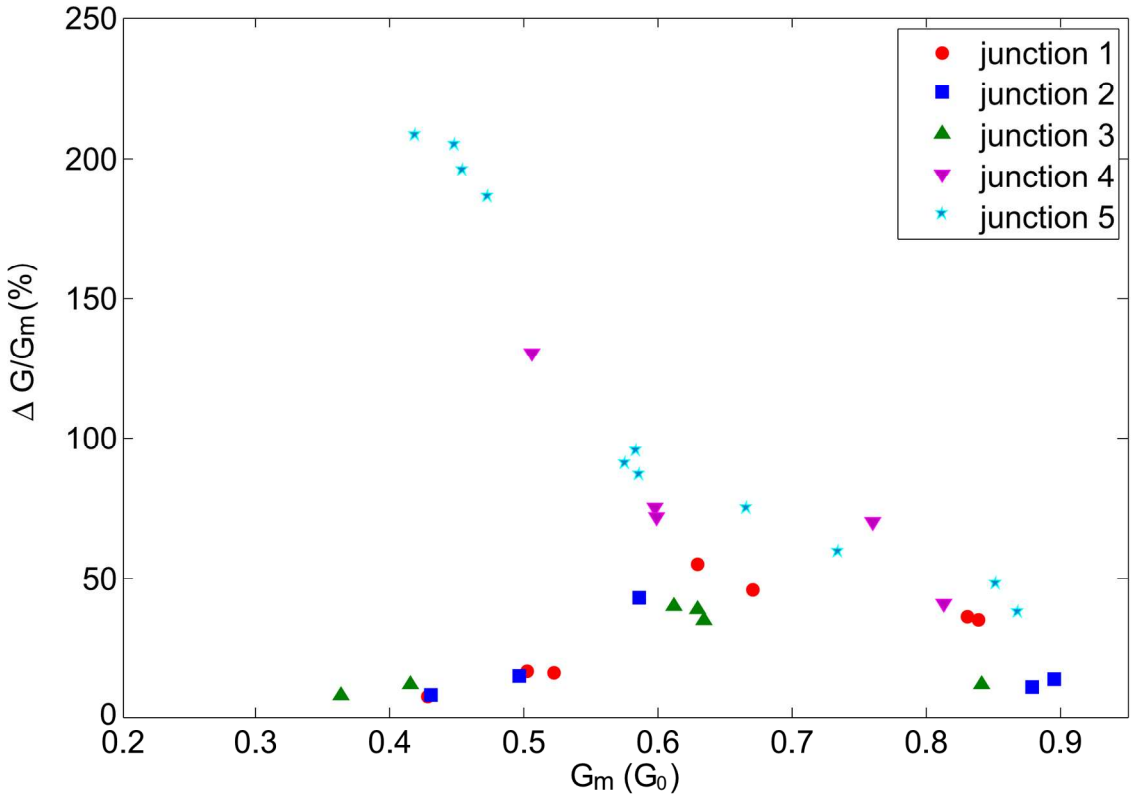

Figure S5: The dependence of AMR on junction elongation for different Ni-benzene junctions.

The monotonic behavior of other junctions (such as junctions 4 and 5) may result from premature breaking of the junction during the elongation process before the extended configurations were reached.

VII. Computational Methodology

All calculations were carried out within the framework of density functional theory (DFT)[15], using the generalized –gradient approximation of Perdew, Burke, and Ernzerhof (PBE)[16]. All work has been performed using the VASP plane wave code[17], with a plane wave cut off energy of 550eV. Ion-electron interaction was treated by means of the projector augmented wave method[18,19]. Fermi-Dirac occupation "smearing" over an energy equivalent to 20meV was used to accelerate convergence. An orthogonal super-cell of dimensions 24x24x48 $Å^3$, with single k-point sampling, was used throughout. This allows for the description of a finite system despite the periodic boundary condition as it affords a vacuum of ~10-12 Å between system images, which was found to be sufficient for keeping spurious interactions between system replicas at a negligible level. Geometry optimization was performed until all force components were smaller than $5x10^{-3}$ eV/Å.

VIII. Details of the Model System

The computed model system consisted of two Ni electrodes, oriented along the (111) direction of a face-centered cubic (FCC) lattice and bridged by a benzene molecule, as shown in Fig. S6. Convergence with the number of atomic Ni planes, *n,* was explicitly verified, with *n*=5 used. Junction elongation was simulated by varying the electrode separation while keeping the unit cell dimension constant. Electrode separation was defined as the normal distance between the planes containing the three atoms located immediately behind the apex atom of each electrode. The positions of the apex Ni atoms and the atoms forming the benzene molecule were then optimized without symmetry constraints. Electrode separation was varied between 6.8 Å and 8.3 Å. We found that a separation of 7.2 Å is the lowest energy configuration. At the lowest energy separation, the benzene molecule was found to be normal to the inter-electrode axis. For inter electrode separation beyond 7.5 Å, tilting from the position was increasingly observed.

IX. Charge transfer between molecule and electrodes

We computed the *z* (inter-electrode axis)-distribution of the *xy*-averaged valence charge density difference between one Ni-electrode with the benzene molecule, $\rho_{Elec}(x,y,z)$, and the benzene molecule alone, $\rho_B(x,y,z)$, in the form: $\rho_d(z) = \iint_{-\infty}^{\infty}(\rho_{Elec}(x,y,z) - \rho_B(x,y,z))\,dx\,dy$[20], as a function of the distance along the axis of the electrode. The integration limits were set to the end points of the unit cell along the *x* and *y* directions. The result is shown in Fig. S7. For each atomic layer of the electrode, a peak at the corresponding *z* coordinate value is observed. The benzene molecule plane is at a distance of 19 Å along the *z* axis and shows no significant signature of charge density difference. Because the PBE exchange-correlation functional used here typically overestimates charge transfer[21], these results can be viewed as an upper bound charge, which means that charge transfer from electrode to molecule can be ruled out for all practical purposes.

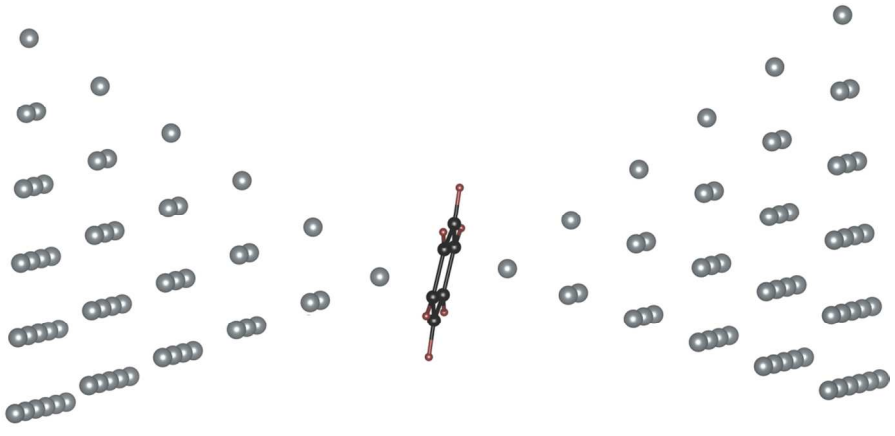

Figure S6: Schematic diagram of the model system used in the computational work.

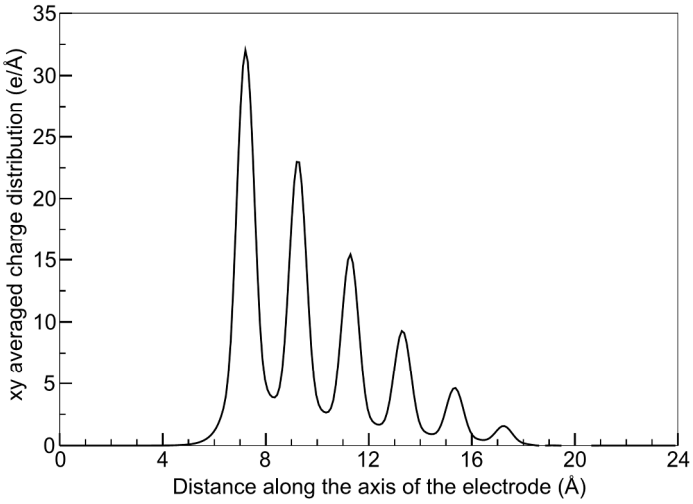

Figure S7: Plane-averaged valence charge density difference as a function of distance along the electrode axis.

X. Real-space plot of the spin-resolved charge density

The real space distribution of charge density, obtained from states residing within an "energy window" of 100 meV around the Fermi energy is plotted for up spin channel in Fig. S8, with an iso-surface value of 0.001 eÅ^{-3}, which is much lower than that used in the main text – 0.007 eÅ^{-3}. At this very low iso-surface value, one can see some contribution at the benzene molecule. But, interestingly, the charge density resembles σ states more than π states. This further makes the point of spin-selective electron transport, because the spin-polarized π states, discussed in the main text as supporting transport, are in the down-spin channel.

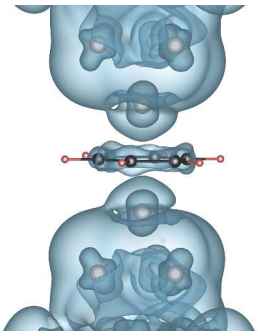

Figure S8: Charge density distribution in real space, collected from orbitals within an energy window of 100 meV around the Fermi energy for the spin-up channel, based on a calculation at equilibrium tip separation of 7.2 Å.

References

[1]Cullity, B. D., Graham, C.D, *Introduction to Magnetic Materials* (Wiley, New jersey 2009).

[2]Egelhoff, W.F. *et. al.,* Artifacts that mimic ballistic magnetoresistance*. J. Magn. Magn.Mater.*, **287**. 496 (2005).

[3]Häfner, M., Viljas, J. K., and Cuevas, J. C., Theory of anisotropic magnetoresistance in atomic-sized ferromagnetic metal contacts. *Phys. Rev. B,* **79**, 140410 (2009).

[4]Gabureac, M., Viret, M., Ott, F., and Fermon, C., Magnetoresistance in nanocontacts induced by Magnetostrictive effects. *Phys. Rev. B*, **69**, 100401 (2004).

[5]Keane, Z. K., Yu, L. H., and Natelson, D., Magnetoresistance of atomic-scale electromigrated nickel nanocontacts. *Appl. Phys. Lett.,* **88**, 062514 (2006).

[6]Bolotin, K. I., Kuemmeth, F. and Ralph, D. C., Anisotropic Magnetoresistance and Anisotropic Tunneling Magnetoresistance due to Quantum Interference in Ferromagnetic Metal Break Junctions. *Phys. Rev. Lett.,* **97**, 127202 (2006).

[7]Shi, S.-F., Bolotin, K. I., Kuemmeth, F., and Ralph, D. C., Temperature dependence of anisotropic magnetoresistance and atomic rearrangements in ferromagnetic metal break junctions. *Phys. Rev. B*, **76**, 184438 (2007).

[8]Giddings, A. D. *et. al.,* Large Tunneling Anisotropic Magnetoresistance in (Ga,Mn)As Nanoconstrictions. *Phys. Rev. Lett.* **94**, 127202 (2005).

[9]Vila, L., Piraux, L., George, J. M., and Faini, G., Multiprobe magnetoresistance measurements on isolated magnetic nanowires. *Appl. Phys. Lett.,* **80**, 3805 (2002).

[10]Weileret, M. *et al.*, Voltage controlled inversion of magnetic anisotropy in a ferromagnetic thin film at room temperature, New J. of Phys., **11**, 013021(2009).

[11]Naidyuk, Y. G. and Yanson, I. K., *Point-contact spectroscopy*, vol. 145, (Springer, 2005).

[12]Kiguchi, M., *et. al.* Highly Conductive Molecular Junctions Based on Direct Binding of Benzene to Platinum Electrodes. *Phys. Rev. Lett.,* **101**, 046801 (2008).

[13]Kaneko, S., Nakazumi, T., and Kiguchi, M., Fabrication of a Well-Defined Single Benzene Molecule Junction Using Ag Electrodes. *J. Phys. Chem. Lett.,***1**, 3520 (2010).

[14]Stipe, B. C., Rezaei, M. A., and Ho, W., Single-Molecule Vibrational Spectroscopy and Microscopy. *Science,* **280**, 1732 (1998).

[15]Parr, R. G., and Yang, W., *Density-Functional Theory of Atoms and Molecules,* (Oxford University Press, 1989).

[16]Perdew, J. P., Burke, K., and Ernzerhof, M., Generalized Gradient Approximation Made Simple. *Phys. Rev. Lett.***77**, 3865 (1996).

[17]Kresse, G., and Furthmüller, J., Efficient iterative schemes for *ab initio* total-energy calculations using a plane-wave basis set. *Phys. Rev. B*, **54**, 11169 (1996).

[18]Blöchl, P. E., Projector augmented-wave method. *Phys. Rev. B,* **50**, 17953 (1994).

[19]Kresse, G.,and Joubert, D., From ultra-soft pseudopotentials to the projector augmented-wave method. *Phys. Rev. B,* **59**, 1758 (1999).

[20]Deutsch, D., Natan, A., Shapira, Y., and Kronik, L., Electrostatic Properties of Adsorbed Polar Molecules: Opposite Behaviour of a Single Molecule and a Molecular Monolayer. *J. Am. Chem. Soc.,* **129**, 989 (2007).

[21]Kümmel, S., and Kronik, L., Orbital-dependent density functionals: Theory and applications. *Rev. Mod. Phys.***, 80**, 3 (2008).